Three-dimensional Holographic Vector of Atomic Interaction Field (3D-HoVAIF) for the QSPR/QSAR of Polychlorinated Naphthalenes①

LI Zheng-Hua CHEN Gang CHEN Zhi-Tao
XIA Zhi-Ning② CHENG Fan-Sheng CHEN Hua
(*College of Chemistry and Chemical Engineering, Chongqing University, Chongqing* 400030*, China*)

ABSTRACT Three-dimensional holographic vector of atomic interaction field (3D-HoVAIF) is used to describe the chemical structures of polychlorinated naphthalenes (PCNs). After variable screening by stepwise multiple regression (SMR) technique, the liner relationships between gas-chromatographic relative retention time (*RRT*), 298 K supercooled liquid pressures (logP_L), *n*-octanol/air partition coefficient (logK_{OA}), *n*-octanol/water partition coefficient (logK_{OW}), aqueous solubilities (logS_W), relative in vitro potency values (–log*EROD*) of PCNs and 3D-HoVAIF descriptors have been established by partial least-square (PLS) regression. The result shows that the 3D-HoVAIF descriptors can be well used to express the quantitative structure-property (activity) relationships of PCNs. Predictive capability of the models has also been demonstrated by leave-one-out cross-validation. Moreover, the predicted values have been presented for those PCNs which are lack of experimentally physico-chemical properties and biological activity by the optimum models.

Keywords: polychlorinated naphthalenes, three-dimensional holographic vector of atomic interaction field, QSPR, QSAR

1 INTRODUCTION

Polychlorinated naphthalenes (PCNs) are an important type of environmentally persistent pollutants and have always attracted great attention[1]. PCNs have been frequently found in several matrices including sediments[2-3], soils[4], water[2], air[5-6], biota[7] and even food and dietary exposure[8]. The toxicologic studies have shown that PCNs have similar toxic properties to polychlorinated dibenzo-*p*-dioxins (PCDDs), polychlorinated dibenzofurans (PCDFs) and polychlorinated biphenyls (PCBs), such as the induction of aryl hydrocarbon hydroxylase (AHH)[9-10] and 7-ethoxyresorufin-O-deethylase (EROD)[10] activity which are important for the hepatic drug-metabolising activity. In addition, the effect of PCNs on GABA-metabolizing enzymes[11] and cytochrome P-450[12] has been investigated.

Physico-chemical properties of an organic chemical compound are often the key role in assessing its distribution and transport in the global environment, such as vapour pressures (P_L), water solubility (S_W), *n*-octanol/air partition coefficients (K_{OA}) and *n*-octa-

Received 30 May 2011; accepted 14 November 2011
① This work was supported by the Ministry of Science and Technology of China (2010DFA32680), the National Natural Science Foundation of China (21005062) and the Fundamental Research Funds for the Central Universities (CDJRC10220010)
② Corresponding author. Xia Zhi-Ning, PhD, Professor. E-mail: chem_lab_cqu@yahoo.com.cn

nol/water partition coefficients (K_{OW}). Moreover, various biological activities play an important role in evaluating the integrated risk for adverse human health effect and environment risk assessment. There is the presence of 76 theoretically possible isomers for PCNs depending on the number and substitution pattern of chlorine atoms. Not only owing to the time consuming and high expense, but also to the lack of PCNs standards, it is hard to determine experimentally the physico-chemical properties and various biological activities for all PCNs. Therefore, alternative approaches are needed. Many previous studies[13-16] indicated that it is a feasible and effective approach to predict the physico-chemical proprieties and biological activity of many organic compounds by quantitative structure-property (activity) relationship (QSPR/QSAR) models. Actually, the QSPR/QSAR studies on PCNs have been reported in recent literatures[17-20], but most of these studies just focused on one or few properties.

In the QSPR and QSAR studies, people always have a profound interest in the choice of appropriate structural parameters. Presently, the common molecular structure descriptors can be divided into 2D and 3D types. However, 2D descriptors are impossible to take reappearance of molecular actual spatial structures and regardless of the molecular interactions. Under such circumstances, 3D descriptors have been progressively developed in structural representation. For example, CoMFA and the similar method, CoMSIA, have been applied to study the persistent organic pollutants (POPs) screening for atmosphere persistence[14] and the toxicity of polybrominated diphenylethers (PBDEs)[21]. However, these methods suffer from the intrinsic unfavorable drawback of strong reliance on molecular conformation, complicated calculation, and so on. Three-dimensional Holographic Vector of Atomic Interaction Field (3D-HoVAIF) is a new 3D descriptor based on the 2D molecular structure characterization method proposed by Li and his co-workers[22-24], including merits of both traditional 2D and 3D descriptors (2D are easy and rapid for calculations and 3D is more amenable to physico-chemical interpretations). Based on the two space invariants (atomic relative distance and atomic properties) and three kinds of non-bonded interaction modes, the 3D-HoVAIF method derives multi-dimensional vectors to represent molecular structural characteristics and is independent of experiments. In this paper, we report six quantitative structure-property (activity) relationships of PCNs established by using the 3D-HoVAIF descriptors. It can help us gain insight into how the physico-chemical properties and biological activity are affected by the 3D-HoVAIF descriptors, and provide a new method for predicting physicochemical properties and biological activities of PCNs.

2 MATERIALS AND METHODS

2.1 Data set

All experimentally determined physico-chemical properties and biological activities of PCNs were taken from previous publications, including *RRT*[17], $\log P_L$[25], $\log K_{OA}$[26], $\log K_{OW}$[27], $\log S_W$[28] and $-\log EROD$[29-30] of PCNs. All the values in this study are listed in Table S1 of the Supplementary materials.

2.2 Three-dimensional holographic vector of atomic interaction field

2.2.1 Atomic types and interactions

As is well known, ordinary atoms of organic molecules including H, C, N, P, O, S, Cl, Br and I are partitioned into 5 types in the Periodic Table of elements. According to hybridization sate of atoms, these atoms are furthermore subdivided into 10 tapes. Therefore, there are 55 interatomic interactions in a molecule (Table 1). In this paper, three kinds of potential energy, electrostatic, steric and hydrophobic, take part in the representation of different interactions, producing $3 \times 55 = 165$ interaction items for the organic compounds.

2.2.2 Electrostatic interaction

Electrostatic interaction, an important non-bonded interaction, could be expressed by classical Coulomb

theorem (Eq. 1).

$$E_{mn}(E) = \sum_{i=m,j=n} \frac{e^2}{4\pi\varepsilon_0}\frac{Z_i Z_j}{r_{ij}}$$

$(1 \leqslant m \leqslant 10, m \leqslant n \leqslant 10)$ (1)

where r_{ij} is the interatomic Euclid distance (nm), the unit electric charge of 1.6021892×10^{-19}C, ε_0 the vacuum dielectric constant being $8.85418782 \times 10^{-12}C^2/J\cdot m$, Z the amounts of net electric charges, and m and n are atomic types. All electrostatic interaction descriptors are calculated by this formula.

2. 2. 3 Steric interaction

Steric interaction describing the interatomic spatial nondipole-dipole or dipole-induced interactions is expressed by Lennard-Jones (Eq. 2).

$$E_{mn}(S) = \sum_{i=m,j=n}\varepsilon_{ij} D\left[\left(\frac{R^*_{ij}}{r_{ij}}\right)^2 - 2\left(\frac{R^*_{ij}}{r_{ij}}\right)^6\right]$$

$(1 \leqslant m \leqslant 10, m \leqslant n \leqslant 10)$ (2)

where $\varepsilon_{ij} = (\varepsilon_{ii}\cdot\varepsilon_{jj})^{1/2}$ is potential well of atomic pairs cited form literatures[31-32]. D is empirical atomic interaction correction constant (0.01)[39]. $R^*_{ij} = (C_h\cdot R^*_{ii} + C_h\cdot R^*_{jj})/2$ is van der Waals' radius for modified atom-pair, with corrected factor Ch of 1.00 in case of sp^3 hybridization, 0.95 sp^2 hybridization and 0.90 sp hybridization[33].

2. 2. 4 Hydrophobic interaction

Hydrophobic interaction force field is defined as interatomic hydrophobic interaction in hint method proposed by Kellogg[34] (Eq. 3).

$$E_{mn}(H) = \sum_{i=m,j=n} S_i a_i S_j a_j e^{-r_{ij}} T_{ij}$$

$(1 \leqslant m \leqslant 10, m \leqslant n \leqslant 10)$ (3)

where H is the solvent accessible surface area for atoms[35], indicating formation on surface area when water-molecule probes the roiling sphere at the atomic surface; a is the atomic hydrophobic constant cited from the reference[36]; T is the sign function, indicating entropy change resulting from different types of atomic interaction[34].

3 RESULTS AND DISCUSSION

3. 1 Structure characterization

Original spatial structures of the 76 PCNs molecules are autogenerated by software Chemoffice 8.0, and then optimized preliminarily using semi-empirical quantum chemistry soft MOPAC in Chem 3D at the AM1 level (energy cut-off: 0.001 $kJ\cdot mol^{-1}$). Simultaneously, atomic partial charges were calculated by Mülliken population analysis at the single-point. Taking forms of Cartesian coordinates and partial charges respectively, spatial position for each atom in a molecule and the atomic charges were input into the C-edited program 3D-HoVAIF, giving rise to 3D-HoVAIF descriptors of the molecule. Comprising 3 atom types as H, $C_{(SP^2)}$ and Cl in the PCNs, 147 empty items were found in the above-mentioned 165 3D-HoVAIF descriptors. Removing all the empty items, there are ultimately 18 3D-HoVAIF descriptors corresponding to a molecule (For details, see Table S2 in the supporting document).

Firstly, correlation between the 3D-HoVAIF descriptors of PCNs and the physico-chemical properties and biological activity was established by PLS regression. Of that, PLS introduce variables in turn according to the values of Fisher prominent test by stepwise multiple regression (SMR) analysis by SPSS 13.0. The predictive power of the QSPR/QSAR model was validated by leave-one-out cross-validated (LOO-CV) analysis. The optimum variable number is determined in case the cross-validated correlative coefficient was getting to the maximum. It is noteworthy that the PLS latent variable number for each original variable matrix in PLS was determined by default standards in Simca-P 10.0. Moreover, NIPALS iteration was performed on principal components one by one based on the square error of original variables and then their contribution to Q^2cum in LOO-CV was tested. If its Q^2cum is smaller than 0.097, the principal component was believed to be insignificant and eliminated.

3. 2 Model foundation and analysis

The variable selection by SMR and the statistic of the models between 3D-HoVAIF descriptors and the physico-chemical properties and biological activity established by PLS were collected in Table S3-S8 of the supplementary materials. Table 2 summarizes the optimum QSPR and QSAR models for PCNs, in which N represents the number of data points submitted to the regression, PC the number of principal constituents, R the correlation coefficient, Q the cross-validated correlation coefficient, and RMSEE the fitted root-mean-square error of estimation.

3. 2. 1 QSPR model of *RRT*

The optimum QSPR model of RRT includes four variables: hydrophobic interaction items V_{113}, V_{120}, V_{137}, and electrostatic interaction item V_3. This model adopts one significant principal component explaining 99.01% variance (R^2) of dependent variable, whose cross-validation variance of dependent variable (Q^2) is 98.95%, and the fitted root-mean-square error of estimation (RMSEE) is 23.8923. The result shows the model exhibits excellent prediction ability and stability, which is similar to other estimation models found by Oliveron *et al.*[17], Zhai *et al.*[18] or Xu *et al*[19]. The plot predicted by the optimum QSPR models and observed *RRT* values is shown in Fig. 1(a).

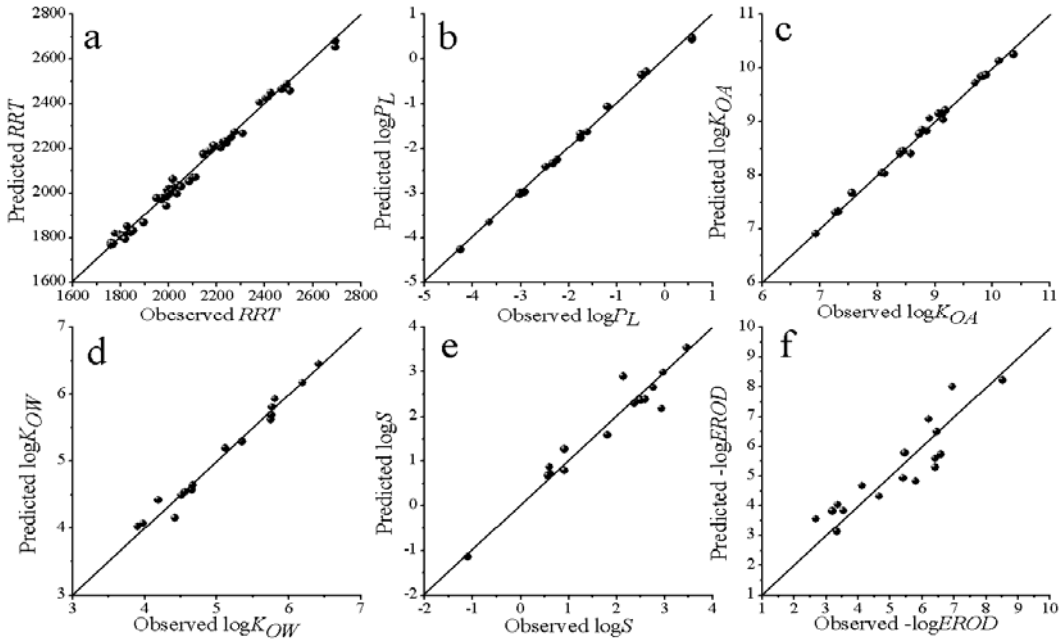

Fig. 1. Plot of the observed and predicted physico-chemical properties and biological activity values of PCNs by the optimum models

With further analysis of this model, V_3 means the electrostatic interaction between sp^2 hybrid C and H atoms, V_{113} represents the hydrophobic interaction between sp^2 hybrid C and H atoms, V_{120} is the hydrophobic interaction of H and Cl atoms, and V_{137} shows the hydrophobic interaction of sp^2 hybrid C and Cl atoms. The values of variables important in projection (VIP) of these four variables are V_{113} 1.11898, V_{137} 1.1172, V_2 1.11226 and V_{120} 0.512417. It makes clear that hydrophobic interaction has the most effect on the gas-chromatographic relative retention time of PCNs, and electrostatic interaction has the secondary impact.

3. 2. 2 QSPR model of logP_L

The optimum QSPR models of logP_L are deemed to be created by SMR-PLS method with 3 independent variables, i.e., electrostatic interaction item V_{20} and steric interaction items V_{56}, V_{58}. This model just adopts two principal components explaining 99.72% square error of Y variable and 99.66% in cross-validation, which suggests that it uses 3D-HoVAIF descriptors superior in both internal estimation ability and external predictabilities compared with the models established by Puzyn *et al.*[20] (R^2 =

0.994, Q^2 = 0.990). The plot predicted by the optimum QSPR models and observed logP_L values are shown in Fig. 1(b).

The best SMR-PLS model equation (Eq. 2) was selected for further analysis. In this model, V_{58} means steric interaction between the sp^2 hybrid C and H atoms, V_{56} represents the steric interaction between H and H atoms, V_{20} stands for the electrostatic interaction of sp^2 hybrid C and sp^2 hybrid C atoms, and so on. The values of VIP of these three variables are V_{58} 1.02292, V_{20} 1.00199 and V_{56} 0.974501, respectively, so the steric interaction has the most effect on the vapour pressures of PCNs, and electrostatic interaction has the secondary impact.

3. 2. 3 QSPR model of logK_{OA}

The optimum QSPR model of logK_{OA} by SMR-PLS includes 4 independent variables: V_3, V_{10}, V_{58}, V_{165}, and 2 principal components explaining 99.35% variance of the Y variables in contrast with 99.10% by the cross-validation. It exhibits a good prediction ability and stability, similar to the model found by Puzyn *et al*.[20] (R^2 = 0.999, Q^2 = 0.988). Fig. 1(c) shows the plot predicted by the optimum QSPR models and observed logK_{OA} values.

We select the best SMR-PLS model equation (Eq. 3) for further analysis. In this model, V_3 means the electrostatic interaction between sp^2 hybrid C and H atoms, V_{10} represents the electrostatic interaction between H and Cl atoms, V_{58} is the steric interaction between sp^2 hybrid C and H atoms, V_{165} stands for the hydrophobic interaction of Cl and Cl atoms, *etc*. The values of VIP of these four variables are V_{165} 1.03554, V_{58} 1.00156, V_3 0.995346 and V_{10} 0.966346, as we can find that hydrophobic interaction has the most effect on vapour pressures of PCNs, and steric and electrostatic interactions have the secondary impact.

3. 2. 4 QSPR model of logK_{OW}

The optimum QSPR model of logK_{OW} includes six variables, i.e., electrostatic interaction items V_1, V_{20}, steric interaction items V_{58}, V_{65}, V_{82}, and hydrophobic interaction item V_{165}. This model uses two significant principal components to explain 97.91% variance of the Y variable, whose cross-validation variance of Y is 95.59%, and the RMSEE is 0.1362. It also exhibits good prediction ability and stability, which is better than the model established by Puzyn *et al*.[37] (R^2 = 0.932, Q^2 = 0.981). Fig. 1(d) presents the plot predicted by the optimum QSPR model and observed logK_{OW} values.

In the optimum model, V_1 stands for the electrostatic interaction between H and H atoms, V_{20} means the electrostatic interaction of sp^2 hybrid C and sp^2 hybrid C atom, V_{58} is the steric interaction of sp^2 hybrid C and sp^2 hybrid C atoms, V_{65} represents the steric interaction of H and H atoms, V_{82} stands for the steric interaction of sp^2 hybrid C and Cl atoms, and V_{165} shows the hydrophobic interaction of Cl and Cl atoms. The values of VIP of these six variables in sequence are V_{20} 1.22202, V_1 1.16178, V_{85} 1.07558, V_{58} 1.05911, V_{165} 0.816118 and V_{65} 0.460778. Conclusion could be drawn that the electrostatic interaction and steric interaction items are more significant and contribute more to the logK_{OW} of PCNs, especially the electrostatic interaction items, and the hydrophobic interaction items are less influential for the logK_{OW} of PCNs.

3. 2. 5 QSPR model of log$S$

The optimum model includes four variables, i.e., electrostatic interaction items V_1 and V_3 together with steric interaction items V_{82} and V_{110}. This model adopts three significant principal components to explain 93.11% variance of Y variables in contrast with 91.05% by cross-validation. The result shows this model exhibits quite satisfactory prediction ability and stability. In fact, this model is similar to the models constructed by Puzyn *et al*.[38]. The plot predicted by the optimum QSPR model and observed log$S$ values are presented in Fig. 1(e).

In the optimum model, V_1 means the electrostatic interaction of H and H atoms, V_3 is the electrostatic interaction of sp^2 hybrid C and H atoms, V_{82} stands for the steric interaction of sp^2 hybrid C and Cl atoms, and V_{110} represents the steric interaction of Cl and Cl atoms. The values of VIP of these six variables in sequence are V_{82} 1.10107, V_3 1.0676, V_1

1.06147 and V_{110} 0.72191. The fact that the most contributive top four items including two electrostatic interaction items and two steric interaction items indicated an intimate relationship between the logarithm of aqueous solubility for PCNs, especially the steric interactions. Here the hydrophobic interaction items are not introduced.

3. 2. 6 QSAR model of –log*EROD*

The optimum model just includes one variable, electrostatic interaction item V_{27}, which can explain 81.94% variance of Y variables in contrast with 79.36% by cross-validation. Although low, the cross-validated Q^2 validation of this model is above 0.50, which indicates the model has an acceptable level of prediction ability and stability. This model is similar to that established by Falandysz *et al*.[39] (R^2 = 0.823). The plot predicted by the optimum QSAR model and observed –log*EROD* values is presented in Fig. 1(f).

In this model, V_{27} means electrostatic interaction of sp^2 hybrid C and Cl atoms, so we can find the electrostatic interaction has most effect on the induction of ethoxyresorufin *O*-deethylase (EROD) for PCNs.

Hence, we take the optimum models to predict the *RRT*, logP_L, logK_{OA}, logK_{OW}, log*S* and –log*EROD* values for all PCNs. The predicted values for all PCNs, including those whose experimentally determined physico-chemical properties and biological activity are unavailable, are listed in Table S1 of the supplementary materials.

Table1. Ten Atomic Types and Their 55 Types of Atomic Interactions in 3D-HoVAIF[a]

No.	Atoms types	1	2	3	4	5	6	7	8	9	10
1	H	V_{1+55n}	V_{2+55n}	V_{3+55n}	V_{4+55n}	V_{5+55n}	V_{6+55n}	V_{7+55n}	V_{8+55n}	V_{9+55n}	V_{10+55n}
2	$C_{(SP^3)}$		V_{11+55n}	V_{12+55n}	V_{13+55n}	V_{14+55n}	V_{15+55n}	V_{16+55n}	V_{17+55n}	V_{18+55n}	V_{19+55n}
3	$C_{(SP^2)}$			V_{20+55n}	V_{21+55n}	V_{22+55n}	V_{23+55n}	V_{24+55n}	V_{25+55n}	V_{26+55n}	V_{27+55n}
4	$C_{(SP)}$				V_{28+55n}	V_{29+55n}	V_{30+55n}	V_{31+55n}	V_{32+55n}	V_{33+55n}	V_{34+55n}
5	$N/P_{(SP^3)}$					V_{35+55n}	V_{36+55n}	V_{37+55n}	V_{38+55n}	V_{39+55n}	V_{40+55n}
6	$N/P_{(SP^2)}$						V_{41+55n}	V_{42+55n}	V_{43+55n}	V_{44+55n}	V_{45+55n}
7	$N/P_{(SP)}$							V_{46+55n}	V_{47+55n}	V_{48+55n}	V_{49+55n}
8	$O/S_{(SP^3)}$								V_{50+55n}	V_{51+55n}	V_{52+55n}
9	$O/S_{(SP^2)}$									V_{53+55n}	V_{54+55n}
10	F, Cl, Br, I										V_{55+55n}

[a] n = 0, the electrostatic interaction items; n = 1, the steric interaction items; n = 2, the hydrophobic interaction items

Table 2. Fitting Results for the Optimum Models by SMR-PLS

No.	Equations	N	PC	R^2	Q^2	RMSEE
1	$RRT = 8.829 + 0.314V_3 + 0.316V_{113} - 0.145V_{120} - 0.315V_{137}$	62	1	0.9901	0.9895	23.8925
2	$\log P_L = -1.388 + 0.443V_{20} + 0.207V_{56} + 0.756V_{58}$	17	2	0.9972	0.9966	0.0788
3	$\log K_{OA} = 9.481 + 0.169V_3 + 0.055V_{10} + 0.215V_{58} - 0.579V_{165}$	24	2	0.9935	0.9910	0.0780
4	$\log K_{OW} = 6.271 - 3.354V_1 + 3.866V_{20} - 0.072V_{58} - 0.101V_{65} + 1.764V_{82} +$	16	4	0.9791	0.9559	0.1362
5	$\log S = 1.380 - 0.516V_1 + 0.323V_3 - 2.097V_{82} + 0.458V_{110}$	15	3	0.9311	0.9105	0.3731
6	$-\log EROD = 3.183 + 0.905V_{27}$	17	1	0.8194	0.7936	0.7228

4 CONCLUSION

Quantitative structure-property (activity) relationships for *RRT*, logP_L, logK_{OA}, logK_{OW}, logS_W and –log*EROD* of PCNs have been established with good correlation coefficients and cross-validated correlation coefficients. It has been shown that the models have good prediction capability and favourable stability and 3D-HoVAIF descriptors can be well used to characterize the molecular structure information and express the quantitative structure-property (activity) relationships of PCNs.

REFERENCES

(1) Falandysz, J. Polychlorinated naphthalenes: an environmental update. *Environ. Pollut*. **1998**, 101, 77–90.

(2) Ishaq, R.; Persson, N. J.; Zebühr, Y.; Broman, D. PCNs, PCDD/Fs, and non-ortho PCBs, in water and bottom sediments from the industrialized norwegian grenlandsfjords. *Environ. Sci. Technol*. **2009**, 43, 3442–3447.

(3) Brack, W.; Bláha, L.; Giesy, J. P.; Grote, M.; Moeder, M.; Schrader, S.; Hecker, M. Polychlorinated naphthalenes and other dioxin-like compounds in Elbe river sediments. *Environ. Toxicol. Chem*. **2008**, 27, 519–528.

(4) Krauss, M.; Wilcke, W. Polychlorinated naphthalenes in urban soils: analysis, concentrations, and relation to other persistent organic pollutants. *Environ. Pollut*. **2003**, 122, 75–89.

(5) Lee, S. C.; Harner, T.; Pozo, K.; Shoelb, M.; Muir, D. C. G.; Barrie, L.; Jones, K. Polychlorinated naphthalenes in the global atmospheric passive sampling (GAPS) study. *Environ. Sci. Technol*. **2007**, 41, 2680–2687.

(6) Herbert, B. M. J.; Halsall, C. J.; Villa, S.; Fitzptricka, L.; Jones, K. C.; Lee, R. G. M.; Kallenborn, R. Polychlorinated naphthalenes in air and snow in the Norwegian Arctic: a local source or an Eastern Arctic phenomenon? *Sci. Total. Environ*. **2005**, 342, 145–160.

(7) Villeneuve, D. L.; Kannan, K.; Khim, J. S.; Nikiforov, V. A.; Blankenship, A. L.; Giesy, J. P. Relative potencies of individual polychlorinated naphthalenes to induce dioxin-like responses in fish and mammalian InVitro bioassays. *Arch. Environ. Contam. Toxicol.* **2000**, 39, 273–281.

(8) Fernandes, A.; Mortimer, D.; Gem, M.; Smith, F.; Rose, M.; Panton, S.; Carr, M. Polychlorinated naphthalenes (PCNs): congener specific analysis, occurrence in food, and dietary exposure in the UK. *Environ. Sci. Technol*. **2010**, 44, 3533–3538.

(9) Blankenship, A. L.; Kannan, K.; Villalobos, S. A.; Villeneuve, D. L.; Falandysz, J.; Imagawa, T.; Jakobsson, E.; Giesy, J. P. Relative potencies of individual polychlorinated naphthalenes and halowax mixtures to induce Ah receptor-mediated responses. *Environ. Sci. Technol*. **2000**, 34, 3153–3158.

(10) Engwall, M.; Brunström, B.; Jakobsson, E. Ethoxyresorufin *o*-deethylase (EROD) and aryl hydrocarbon hydroxylase (AHH)-inducing potency and lethality of chlorinated naphthalenes in chicken (Gallus domesticus) and eider duck (Somatera mollissima) embryos. *Arch. Toxicol*. **1994**, 68, 37–42.

(11) Vinitskay, H.; Lachowicz, A.; Kilanowicz, A.; Bartkowiak, J.; Zylinska, L. Exposure to polychlorinated naphthalenes affects GABA-metabolizing enzymes in rat brain. *Environ. Toxicol. Phar.* **2005**, 20, 450–455.

(12) Kilanowicz, A.; Skrzypinska-Gawrysiak, M.; Sapota, A.; Galoch, A.; Daragó, A. Subacute toxicity of polychlorinated naphthalenes and their effect on cytochromeP-450. *Ecotox. Environ. Safe.* **2009**, 72, 650–657.

(13) Xu, H. Y.; Zou, J. W.; Yu, Q. S.; Wang, Y. H.; Zhang, J. Y.; Jin, H. X. QSPR/QSAR models for prediction of the physicochemical properties and biological activity of polybrominated diphenylether. *Chemosphere* **2007**, 66, 1998–2010.

(14) Lv, Y. Y.; Yin, C. S.; Liu, H. Y.; Yi, Z. S.; Wang, Y. 3D-QSAR study on atmospheric half-lives of POPs using CoMFA and CoMSIA. *J. Environ. Sci.* **2008**, 20, 1433–1438.

(15) Gharagheizi, F. A QSPR model for estimation of lower flammability limit temperature of pure compounds based on molecular structure. *J. Hazard. Mater.* **2009**, 169, 217–220.

(16) Xu, H. Y.; Zou, J. W.; Hu, G. X.; Wang, W. QSPR/QSAR models for prediction of the physico-chemical properties and biological activity of polychlorinated diphenylethers (PCDEs). *Chemosphere* **2010**, 80, 665–670.

(17) Olivero, J.; Kannan, K. Quantitative structure-retention relationships of polychlorinated naphthalenes in gas chromatography. *J Chromatogr. A* **1999**, 849, 621–627.

(18) Zhai, Z. C.; Wang, Z. Y.; Chen, S. D. Quantitative structure-retention relationship for gas chromatography of polychlorinated naphthalenes by *ab initio* quantummechanical calculations and a Cl substitution position method. *QSAR Comb. Sci.* **2006**, 25, 7–14.

(19) Xu, H. P.; Chen, X. S.; Li, C. P.; Zhang, J. Y. Predictive and comparative study of chromatographic retention index for 75 chloronaphthalene congeners. *Chin. J. Struct. Chem.* **2009**, 28, 1245–1250.

(20) Puzyn, T.; Falandysz, J. Computational estimation of logarithm of *n*-octanol/air partition coefficient and subcooled vapor pressures of 75 chloronaphthalene congeners. *Atoms. Environ.* **2005**, 39, 1439–1446.

(21) Gu, C. G.; Ju, X. H.; Jiang, X.; Kai, Y.; Yang, S. G.; Sun, C. Improved 3D-QSAR analyses for the predictive toxicology of polybrominated diphenylethers with CoMFA/CoMSIA and DFT. *Ecotox. Environ. Safe.* **2010**, 73, 1470–1479.

(22) Zhou, P.; Tian, F. F.; Li, Z. L. Three-dimensional holographic vector of atomic interaction field (3D-HoVAIF). *Chemom. Intell. Lab. Syst.* **2007**, 87, 88–94.

(23) Jing, J. H.; Liang, G. Z.; Mei, H.; Zhang, Q. X.; Li, Z. L.; Lv, F. L. QSAR studies on influenza neuraminidase inhibitors — acylthiourea analogue.

Chin. J. Struct. Chem. **2009**, 28, 200–204.

(24) Yang, S. B.; Xia, Z. N.; Mei, H.; Pan, Y.; Yang, Q. L.; Xu, L. N.; Li, Z. L. QSAR study on some N-[5-(2-furanyl)-2-methyl-4-oxo-4H-thieno[2, 3-d]pyrimidin-3-yl]-carboxamide and 3-substituted-5-(2-furanyl)-2-methyl-3H-thieno-[2,3-d]pyrimidin-4-ones using three-dimensional holographic vector of atomic interaction field. *Chin. J. Struct. Chem.* **2009**, 28, 1197–1204.

(25) Lei, Y. D.; Wania, F.; Shiu, W. Y. Vapor pressures of the polychlorinated naphthalenes. *J. Chem. Eng. Data* **1999**, 44, 577–582.

(26) Harner, T.; Bidleman, T. F. Measurement of octanol-air partition coefficients for polycyclic aromatic hydrocarbons and polychlorinated naphthalenes. *J. Chem. Eng. Data* **1998**, 43, 40–46.

(27) Opperhuizen, A.; Vander Velde, E. W.; Gobas, F. A. P. C.; Liem, D. A. K.; Vander Steen, J. M. D.; Hutzinger, O. Relationship between biocongentration in fish and steric factor of hydrophobic chemical. *Chemosphere* **1985**, 14, 1871–1896.

(28) Eucken, A.; Hellwege, K. H. *Landolt-Börnstein Zahlenwerte und Funktionenaus Physic, Chemie, Astronomie, Geophysik, Technik, Springer-Verlag*, Berlin **1951**.

(29) Blankenship, A. L.; Kannan, K.; Villalobos, S. A.; Illeneuve, D. L.; Falandysz, J.; Imagawa, T. Jakobsson, E.; Giesy, J. P. Relative potencies of individual polychlorinated naphthalenes and Halowax mixtures to induce Ah receptor-mediated responses. *Environ. Sci. Technol.* **2000**, 34, 3153–3158.

(30) Villeneuve, D. L.; Kannan, K.; Khim, J. S.; Falandysz, J.; Nikiforov, V. A.; Blankenship, A. L.; Giesy, J. P. Relative potencies of individual polychlorinated naphthalenes to induce dioxin-like responses in fish and mammalian in vitro bioassays. *Arch. Environ. Contam. Toxicol.* **2000**, 39, 273–281.

(31) Levitt, M. Protein folding by restrained energy minimization and molecular dynamics. *J. Mol. Biol.* **1983**, 170, 723–764.

(32) Levitt, M.; Perutz, M. F. Aromatic rings act as hydrogen bond acceptors. *J. Mol. Biol.* **1988**, 201, 751–754.

(33) Hahn, M. Receptor surface models. 1. Definition and construction. *J. Med. Chem.* **1995**, 38, 2080–2090.

(34) Kellogg, G. E.; Semus, S. F.; Abraham, D. J. HINT: A new method of empirical hydrophobic field calculation for CoMFA. *J. Comput. Aided Mol. Des.* **1991**, 5, 545–552.

(35) Hasel, W.; Hendrikson, T. F.; Still, W. C. A rapid approximation to the solvent accessible surface areas of atoms. *Tetrahedron Computer Methodology* **1988**, 1, 103–116.

(36) Pei, J. F.; Wang, Q.; Zhou, J. J.; Lai, L. H. Estimating protein-ligand binding free energy: atomic solvation parameters for partition coefficient and solvation free energy calculation. *Proteins* **2004**, 57, 651–664.

(37) Puzyna, T.; Falandysz, J. Octanol/water partition coefficients of chloronaphthalenes. *J. Environ. Sci. Health., Part A* **2005**, 40, 1651–1663.

(38) Puzyna, T.; Mostrag, A.; Falandysza, J.; Kholod, Y.; Leszczynski, J. Predicting water solubility of congeners: Chloronaphthalenes — A case study. *J. Hazard. Mater.* **2009**, 170, 1014–1022.

(39) Falandysza, J.; Puzyn, T. Computational prediction of 7-ethoxyresorufin-O-diethylase (EROD) and luciferase (luc) inducing potency for 75 congeners of chloronaphthalene. *J. Environ. Sci. Health., Part A* **2004**, 9, 1505–1523.